2023

Topologically Optimized Electrodes for Electroosmotic Actuation

Jianwen Sun

Jianyu Zhang

Ce Guan

Teng Zhou

Shizhi Qian
Old Dominion University

See next page for additional authors

Original Publication Citation

Sun, J., Zhang, J., Guan, C., Zhou, T., Qian, S., & Deng, Y. (2023, 2022-08-01). Topologically optimized electrodes for electroosmotic actuation. *Journal of Advanced Manufacturing Science and Technology*, *3*(1), 1-6, Article 2022022. https://doi.org/10.51393/j.jamst.2022022

Journal of
Advanced Manufacturing Science and Technology
jamst@jamstjournal.com；jamst2020@126.com
www.jamstjournal.com

Topologically optimized electrodes for electroosmotic actuation

Jianwen SUN [a,b], Jianyu ZHANG [a], Ce GUAN[a], Teng ZHOU [c], Shizhi QIAN[d], Yongbo DENG [a,*]

[a] *State Key Laboratory of Applied Optics, Changchun Institute of Optics, Fine Mechanics and Physics (CIOMP), Chinese Academy of Sciences,Changchun 130033, China*
[b] *University of Chinese Academy of Sciences, Beijing 100039, China*
[c] *Mechanical and Electrical Engineering College, Hainan University, Haikou 570228, China*
[d] *Department of Mechanical and Aerospace Engineering, Old Dominion University, ECSB 1309, 4700 Elkhorn Ave, Norfolk, VA 23529, USA*

Received 1 August 2022; revised 22 August 2022; accepted 13 September 2022; Available online 19 September 2022

Abstract: Electroosmosis is one of the most used actuation mechanisms for the microfluidics in the current active lab-on-chip devices. It is generated on the induced charged microchannel walls in contact with an electrolyte solution. Electrode distribution plays the key role on providing the external electric field for electroosmosis, and determines the performance of electroosmotic microfluidics. Therefore, this paper proposes a topology optimization approach for the electrodes of electroosmotic microfluidics, where the electrode layout on the microchannel wall can be determined to achieve designer desired microfluidic performance. This topology optimization is carried out by implementing the interpolation of electric insulation and electric potential on the specified walls of microchannels. To demonstrate the capability of this approach, one typical electroosmotic device, i.e., electroosmotic micropump, is modeled with several electrode layouts derived. And this approach permits potential applications in chemicals and biochemistry due to its outstanding capability on determining the performance of electrokinetic microfluidics.

Keywords: Topology optimization; Micropump; Electroosmosis; Microfluidics; Electrode

1. Introduction

Lab on chip has been developed into microfluidic systems for biological and chemical minute laboratories[1-3]. It is often necessary to pump fluids from one part of the device to another, control fluid motion, enhance mixing, and separate fluids, etc. Electroosmosis, particularly suitable for microfluidic devices, provides an attractive approach for manipulating liquids in microdevices, since microdevices operating on this principle do not require any moving parts. And electroosmosis has been researched in the literatures in the field of microfluidics, including the researches on electroosmotic micropumps[4-6] and electroosmotic micromixer[7, 8].

Several researches have been implemented for mathematically modeling electroosmotic microflows by analytical, numerical and experimental approaches[7-13]; shape optimization-based geometrical design of electroosmotic microchannel has been implemented[14,15]; optimization of zeta potential distributions has been performed for minimal dispersion in an electroosmotic microchannel[16], to name the most relevant. In those researches, electrodes play the key role on generating the microfluidic motion, because they induce the external electric field with attracting charges, because they induce external electric field with attracting charges, thereby attracting ions to move tangentially along the microchannel wall, driving fluid motion in the presence of viscous forces. Therefore, reasonable electrode distribution is key for achieving the performance of the electroosmotic microflows. On the researches of electroosmotic electrodes, asymmetric polarization and nonplanar layout has been adopted for electroosmotic micropumping[17, 18]; staggered array of electrodes has been utilized to produce electroosmotic vortices for micromixing[19]; asymmetric electrode pair has been used in electroosmotic microconcentrator[20]; electric potential effect imposed on wall electrodes has been discussed in binary fluids[21]; facing rows of electrodes has been used for remediation of polluted soils by electrokinetic soil flushing[22], to name the most recent. Although those relevant results provided instructions for the control of electroosmosis, limits on determining the electrode distribution still exists in view of lacking generality, flexibility and efficiency because of the dependence on the designers' intuition and lack of objective design basis. Therefore, this paper focuses on the topology optimization approach for the electrodes of electroosmotic microflows to overcome these limits.

* Corresponding author. *E-mail address:* dengyb@ciomp.ac.cn
Peer review under responsibility of Editorial Committee of JAMST
DOI: 10.51393/j.jamst.2022022

The capability of this topology optimization approach is demonstrated by determining the electrodes respectively for the electroosmotic micropumps, because pumping of microfluids is a typical function that can be achieved by electroosmosis. The derived results show that effective actuation of microflows can be achieved by the electrodes derived using the topology optimization approach. And this proposed method permits potential applications in chemicals and biochemistry due to its outstanding capability on determining the performance of electroosmotic microfluidics. In the following, the methodology of the topology optimization approach is presented in Section 2, followed by modeling the electroosmotic micropumps in Section 3; the solving procedure of the topology optimization problems is introduced in Section 4; the derived results are discussed in Section 5; and this paper is concluded in Section 6.

2. Methodology

Electroosmosis is caused by the accumulation of a net electric charge on the solid surface that is in contact with an electrolyte solution[9]. As a result, charges accumulate in the thin liquid layer next to the solid surface. This thin layer is known as the Debye (or double) layer, and its thickness is typically in the magnitude of 10 nm[10]. The electric potential is the largest at the solid surface, decreases linearly with the increase of the distance from the solid surface, and decays rapidly to electric neutrality away from the solid surface. This charge separation next to the solid wall causes either a positive or negative potential difference (i.e., Zeta potential) across the Debye layer. The magnitude of Zeta potential depends on the characteristics of the solid and the liquid. In the presence of an external electric field, the charges in the double layer are attracted to the oppositely charged electrode and drag the liquid along. Therefore, the electric field, through its action on the charges, creates a body force that induces fluid motion. Usually, the Debye layer is much smaller than the feature size of microfluidics, and the thin Debye layer can be approximated to be slip wall with velocity proportional to the tangential component of the external electric field. Therefore, the layout of the electrodes on the lateral walls of microchannel, which modulates the electric field variation, plays the key role on the performance of electroosmotic microfluidics.

Under the assumption that the thickness of the Debye layer is much smaller than the feature size of microfluidics, the Navier-Stokes equations with slip boundary condition at the wall can be used to describe the electroosmotic microfluidics, where the slip velocity satisfies the Helmholtz-Smoluchowski relation, i.e., it is proportional to the tangential component of the electric field intensity imposed by electrodes[11]

$$\begin{cases} \rho \boldsymbol{u} \cdot \nabla \boldsymbol{u} + \nabla \cdot \left[-\eta \left(\nabla \boldsymbol{u} + \nabla \boldsymbol{u}^{\mathrm{T}} \right) + p\boldsymbol{I} \right] = 0 & \text{in } \Omega \\ -\nabla \cdot \boldsymbol{u} = 0 & \text{in } \Omega \\ \boldsymbol{u} = -\mu_{\mathrm{eo}} \left[\nabla V - (\boldsymbol{n} \cdot \nabla V) \boldsymbol{n} \right] & \text{on } \Gamma_{\mathrm{w}} \cup \Gamma_{\mathrm{d}} \end{cases} \tag{1}$$

where $\boldsymbol{u}$,p are the fluid velocity and pressure, respectively; V is the distribution of the external electrical potential imposed by the electrodes;ρ and η are the density and dynamic viscosity of the electrolyte solution, respectively;$\mu_{\mathrm{eo}} = -\epsilon_{\mathrm{r}}\epsilon_0(\xi_0/\eta)$ is the electroosmotic mobility, with ϵ_{r},ϵ_0 and ξ_0 respectively representing the relative permittivity, permittivity of free space and Zeta potential;$\Omega$is the computational domain sketched in Fig. 1, with the inlet boundary Γ_{ip}, wall boundary $\Gamma_{\mathrm{w}} \cup \Gamma_{\mathrm{d}}$ and outlet boundary Γ_{op} satisfying $\Gamma_{\mathrm{ip}} \cup \Gamma_{\mathrm{op}} \cup \Gamma_{\mathrm{w}} \cup \Gamma_{\mathrm{d}}$; the inlet Γ_{ip} and outlet Γ_{op} are a pair of periodic boundaries imposed with periodic condition of the fluidic velocity; $\boldsymbol{n}$ is the outward unitary normal at $\partial\Omega$; Q is the fluid flux imposed on the inlet of the microchannel, V_0 is the electrical potential imposed on the anode and the cathode is connected to ground.

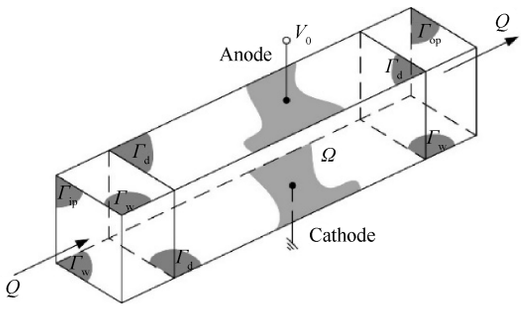

Fig. 1. Sketch of computational domain Ω for electroosmosis.

The distribution of the external electrical potential is described by the Laplace equation. As sketched in Fig.1, the wall boundary is split into two parts, i.e., Γ_{w} and Γ_{d}. For the external electrical potential, Γ_{w} is electric insulation boundary with$-(\sigma\nabla V)\cdot\boldsymbol{n} = 0$; and Γ_{d}, the design domain for the electrodes, is the union of electric insulation and electric potential boundary parts. To distinguish those two types of boundary parts, the variable, nominated physical density, is utilized, and it is valued in [0, 1] with value 0 and 1 respectively representing electric potential and electric insulation boundary types. Then the boundary condition on Γ_{d} can be expressed to be the interpolation of electric insulation and electric potential

$$-(\sigma\nabla V)\cdot\boldsymbol{n} = \alpha\left(V - V_0\right) \quad \text{on } \Gamma_{\mathrm{d}} \tag{2}$$

where σ is electric conductivity; $V_0$is the specified electric potential on the electrodes;$\alpha$is the penalization expressed to be[23]

$$\alpha = \alpha_{\max}\frac{q\left(1-\gamma_{\mathrm{fp}}\right)}{q+\gamma_{\mathrm{fp}}} \tag{3}$$

with γ_{fp}, αmax and q respectively representing the physical density variable, the penalization parameter and the parameter used to tune the convexity of the penalization. The value of αmax should be chosen to be large enough to ensure the domination of the term (V-V_0) in Eq. (2), when the physical density is valued 0. Meanwhile, Eq. (2) degenerates into the electric insulation boundary condition, when the physical density is valued 1. Based on numerical tests, αmax and q are chosen to be 1×10^5 and 1×10^{-3}, respectively. In sum, the external electrical potential can be described to be

$$\begin{cases} -\nabla\cdot(\sigma\nabla V) = 0 & \text{in } \Omega \\ -(\sigma\nabla V)\cdot\boldsymbol{n} = 0 & \text{on } \Gamma_{\mathrm{ip}} \cup \Gamma_{\mathrm{op}} \cup \Gamma_{\mathrm{w}} \\ -(\sigma\nabla V)\cdot\boldsymbol{n} = \alpha(V - V_0) & \text{on } \Gamma_{\mathrm{d}} \end{cases} \tag{4}$$

where the electric insulation boundary condition is imposed on the inlet and outlet of the electroosmotic microflows.

On the physical density variable, it is derived from the design variable defined on Γ_{d}, using the procedure introduced in[24]. The design variable is filtered using the Helmholtz filter to ensure the minimum scale of the implicitly expressed structural layout

$$\begin{cases} -r^2\nabla_{\mathrm{s}}\cdot\nabla_{\mathrm{s}}\gamma_{\mathrm{f}} + \gamma_{\mathrm{f}} = \gamma & \text{in } \Gamma_{\mathrm{d}} \\ -r^2\nabla_{\mathrm{s}}\gamma_{\mathrm{f}}\cdot\boldsymbol{n}_{\mathrm{s}} = 0 & \text{on } \partial\Gamma_{\mathrm{d}} \end{cases} \tag{5}$$

where γ is the design variable,$\gamma_{\mathrm{f}}$is the filtered design variable, ∇_{s} is the gradient operator defined for the local coordinate system on Γ_{d}, r is the filter radius, and $\boldsymbol{n}_{\mathrm{s}}$ is the outward unitary normal on $\partial\Gamma_{\mathrm{d}}$; then the filtered design variable is projected using the threshold method to remove the intermediary values between 0 and 1 and derive the physical density variable

$$\gamma_{\mathrm{fp}}=\frac{\tanh\left(\beta\xi\right)+\tanh\left(\beta\left(\gamma_{\mathrm{f}}-\xi\right)\right)}{\tanh\left(\beta\xi\right)+\tanh\left(\beta\left(1-\xi\right)\right)} \tag{6}$$

where β and ξ are projection parameters. For the value choice of the projection parameters, one can refer to[25].

Based on the above description, the desired performance of the electroosmosis can be derived by topologically optimizing the electrodes of electroosmotic microflows, where the 0−1 distribution of the physical density representing the electrode layout can be determined on Γ_{d} by solving a variational problem corresponding to a specified electroosmotic microdevice.

3. Modeling

Based on the introduced methodology for topology optimization of electrodes for electroosmotic microflows, the electroosmotic pumping is modeled as follows.

Micropumping is an essential function of a microfluidic system[26]. Electroosmotic micropumps are frequently utilized to perform this function, because electroosmotic micropumps possess several outstanding features: electroosmotic micropumps are capable of generating constant and pulse-free flows; the flow magnitude and direction of an electroosmotic micropumps are convenient to control; this type of micropump can be fabricated using standard microfabrication technologies and thus is readily integratable with lab-on-chip devices because of its no-moving-part characteristics[5]. Therefore, this section focuses on topology optimization of the electrodes for electroosmosis to generate the maximal flux in microchannel and achieve the micropumping performance. Then, by setting the flow rate at the ports of electroosmotic microchannel to be the design objective, the variational problem can be constructed to be

$$\max_{\gamma\in[0,1]}\Phi=\frac{1}{\Phi_0}\left(-\int_{\Gamma_{\mathrm{ip}}}u\cdot\boldsymbol{n}\,\mathrm{d}s+\int_{\Gamma_{\mathrm{op}}}u\cdot\boldsymbol{n}\,\mathrm{d}s\right)$$

$$\text{s.t.}\begin{cases}\begin{cases}-\nabla\cdot(\sigma\nabla V)=0 & \text{in }\Omega\\ -(\sigma\nabla V)\cdot\boldsymbol{n}=0 & \text{on }\Gamma_{\mathrm{ip}}\cup\Gamma_{\mathrm{op}}\cup\Gamma_{\mathrm{w}}\\ -(\sigma\nabla V)\cdot\boldsymbol{n}=\alpha(V-V_0) & \text{on }\Gamma_{\mathrm{d}}\end{cases}\\ \begin{cases}\rho\boldsymbol{u}\cdot\nabla\boldsymbol{u}+\nabla\cdot\left[-\eta\left(\nabla\boldsymbol{u}+\nabla\boldsymbol{u}^{\mathrm{T}}\right)+p\boldsymbol{I}\right]=0 & \text{in }\Omega\\ -\nabla\cdot\boldsymbol{u}=0 & \text{in }\Omega\\ \left[-\eta\left(\nabla\boldsymbol{u}+\nabla\boldsymbol{u}^{\mathrm{T}}\right)+p\boldsymbol{I}\right]\boldsymbol{n}=0 & \text{on }\Gamma_{\mathrm{ip}}\cup\Gamma_{\mathrm{op}}\\ \boldsymbol{u}=-\mu_{\mathrm{eo}}\left[\nabla V-(\boldsymbol{n}\cdot\nabla V)\boldsymbol{n}\right] & \text{on }\Gamma_{\mathrm{w}}\cup\Gamma_{\mathrm{d}}\end{cases}\\ \begin{cases}-r^2\nabla_{\mathrm{s}}\cdot\nabla_{\mathrm{s}}\gamma_{\mathrm{f}}+\gamma_{\mathrm{f}}=\gamma & \text{in }\Gamma_{\mathrm{d}}\\ -r^2\nabla_{\mathrm{s}}\gamma_{\mathrm{f}}\cdot\boldsymbol{n}_{\mathrm{s}}=0 & \text{on }\partial\Gamma_{\mathrm{d}}\end{cases}\end{cases} \tag{7}$$

where Φ_0 is the flow rate at the outlet, corresponding to the initial value of the design variable. For solving the PDE constraints of Eq. (7) using the linear element-based finite element method, the weak forms of the PDE constraints are similar with that in equation 1, 4 and 5, except that the boundary integration term on Γ_i is removed from Eq.(1).

To derive the adjoint derivative used for evolving the design variable, the adjoint analysis is implemented for Eq. (7), and the weak forms of the adjoint equations of the Navier-Stokes equations, the electrical potential equation and the Helmholtz filter are derived to be

$$\begin{gathered}\text{Find }\boldsymbol{u}_{\mathrm{a}}\in(H(\Omega))^3,p_{\mathrm{a}}\in L^2(\Omega)\\ \text{and }\lambda_{\mathrm{fa}}\in(H^{-\frac{1}{2}}(\Gamma_{\mathrm{w}}\cup\Gamma_{\mathrm{d}}))^3,\text{satisfying}\\ \int_\Omega\rho\left[(\hat{\boldsymbol{u}}_{\mathrm{a}}\cdot\nabla\boldsymbol{u})\cdot\boldsymbol{u}_{\mathrm{a}}+(\boldsymbol{u}\cdot\nabla\hat{\boldsymbol{u}}_{\mathrm{a}})\boldsymbol{u}_{\mathrm{a}}\right]\\ +\nabla\boldsymbol{u}_a:[\eta(\nabla\hat{\boldsymbol{u}}_a+\nabla\hat{\boldsymbol{u}}_{\mathrm{a}}^{\mathrm{T}})-\hat{p}_{\mathrm{a}}\boldsymbol{I}]-p_{\mathrm{a}}\nabla\cdot\hat{\boldsymbol{u}}_{\mathrm{a}}\mathrm{d}v\\ +\sum_{i=1}^{N_{\mathrm{e}}}\int_{\Omega_i}-\tau_{\mathrm{gls}}\nabla p_{\mathrm{a}}\cdot\nabla\hat{p}_{\mathrm{a}}\mathrm{d}v+\int_{\Gamma_{\mathrm{w}}\cup\Gamma_{\mathrm{d}}}\lambda_{\mathrm{fa}}\cdot\hat{\boldsymbol{u}}_{\mathrm{a}}\\ +(\hat{\lambda}_{\mathrm{fa}}-\hat{p}_{\mathrm{a}}\boldsymbol{n})\cdot\boldsymbol{u}_{\mathrm{a}}\mathrm{d}s+\frac{1}{\Phi_0}\left(-\int_{\Gamma_{\mathrm{ip}}}n\cdot\hat{\boldsymbol{u}}_{\mathrm{a}}\mathrm{d}s+\int_{\Gamma_{\mathrm{op}}}n\cdot\hat{\boldsymbol{u}}_{\mathrm{a}}\mathrm{d}s\right)=0,\\ \forall\hat{\boldsymbol{u}}_{\mathrm{a}}\in(H(\Omega))^3,\forall\hat{p}_{\mathrm{a}}\in L^2(\Omega)\text{ and }\forall\hat{\lambda}_{\mathrm{fa}}\in(H^{\frac{1}{2}}(\Gamma_{\mathrm{w}}\cup\Gamma_{\mathrm{d}}))^3\end{gathered} \tag{8}$$

$$\begin{gathered}\text{find }V_{\mathrm{a}}\in H(\Omega),\text{satisfying}\\ \int_\Omega\sigma\nabla V_{\mathrm{a}}\cdot\nabla\hat{V}_{\mathrm{a}}\mathrm{d}v+\int_{\Gamma_{\mathrm{d}}}\alpha\nabla V_{\mathrm{a}}\cdot\hat{V}_{\mathrm{a}}\mathrm{d}s\\ +\int_{\Gamma_{\mathrm{w}}\cup\Gamma_{\mathrm{d}}}\mu_{\mathrm{eo}}[\nabla\hat{V}_{\mathrm{a}}-(\boldsymbol{n}\cdot\nabla\hat{V}_{\mathrm{a}})\boldsymbol{n}]\cdot\lambda_{\mathrm{fa}}\mathrm{d}s=0,\forall\hat{V}_{\mathrm{a}}\in H(\Omega)\end{gathered} \tag{9}$$

$$\begin{gathered}\text{find }\gamma_{\mathrm{fa}}\in H\left(\Gamma_{\mathrm{d}}\right),\text{satisfying}\\ \int_{\Gamma_{\mathrm{d}}}r^2\nabla_{\mathrm{s}}\gamma_{\mathrm{fa}}\cdot\nabla_{\mathrm{s}}\hat{\gamma}_{\mathrm{fa}}+\gamma_{\mathrm{fa}}\hat{\gamma}_{\mathrm{fa}}+(V-V_0)V_{\mathrm{a}}\frac{\partial\alpha}{\partial\gamma_{\mathrm{fa}}}\frac{\partial\gamma_{\mathrm{p}}}{\partial\gamma_{\mathrm{f}}}\hat{\gamma}_{\mathrm{fa}}\mathrm{d}s=0,\\ \forall\hat{\gamma}_{\mathrm{fa}}\in H\left(\Gamma_{\mathrm{d}}\right)\end{gathered} \tag{10}$$

where $\boldsymbol{u}_{\mathrm{a}},p_{\mathrm{a}},V_{\mathrm{a}}$ and γ_{fa} are the adjoint variables of the corresponding state variables, respectively; λ_{fa} is the adjoint of the Lagrangian multiplier λ_{f}; $\hat{\boldsymbol{u}}_{\mathrm{a}},\hat{p}_{\mathrm{a}},\hat{V}_{\mathrm{a}},\hat{\gamma}_{\mathrm{fa}}$ and $\hat{\lambda}_{\mathrm{fa}}$ are the test functions of the corresponding adjoint variables; $H^{-\frac{1}{2}}(\Gamma_{\mathrm{w}}\cup\Gamma_{\mathrm{d}})$ is the dual space of the trace space $H^{\frac{1}{2}}(\Gamma_{\mathrm{w}}\cup\Gamma_{\mathrm{d}})$. The first-order adjoint derivative of the variational problem in equation 7 is

$$\delta\Phi=\int_{\Gamma_{\mathrm{d}}}-\gamma_{\mathrm{fa}}\delta\gamma\mathrm{d}s \tag{11}$$

In Eq. (11), γ_{fa} is derived by sequentially solving the state equations and the corresponding adjoint equations.

4. Solving

The topology optimization problems for determination of the electrodes for electroosmotic microflows are solved using the iterative approach based on the derived adjoint derivative. The procedure for the iterative approach includes the following steps: (a) the PDE constraints are solved with the current design variable; (b) the adjoint equations are solved based on the solution of the PDE constraints; (c) the adjoint derivative of the design objective is computed; (d) the design variable is updated using the method of moving asymptotes[27]; (e) the convergent criterion are checked to stop the iterative loop, and the procedure will return to (a), if the convergent criterion are not satisfied. The convergent criterion is specified to be that the change of the objective values in five consecutive iterations satisfies $\frac{1}{5}\sum_{i=0}^{4}\left|J_{k-i}-J_{k-i-1}\right|\Big/\left|J_k\right|\leqslant 1\times10^{-3}$ in the $k$thiteration or the maximal iteration number 160 is reached, where J_k is the objective value in the $k$thiteration.

During the iterative procedure, the threshold parameter ξ in equation 6 is set to be 0.5; the initial value of the projection parameter β is set to be 1 and it is doubled every 40 iterations until the preset maximal value 16 is reached; the finite element solving of the partial differential equations and corresponding adjoint equations are implemented in the finite element software COMSOL Multiphysics (http://www.comsol.com), where linear cubic elements are used for all the variables. On the relevant numerical setting, one can refer

to[28] for the more details.

5. Results and discussion

In this section, topology optimization of the electrodes is investigated for electroosmotic micropumps based on the methodology introduced in section 2, to demonstrate the capability of the topology optimization approach for microfluidics. In the following, the liquid of the microflow is the electrolyte with density ρ =1×10^3 kg/m^3, dynamic viscosity η =1×10^{-3} Pa·s, dielectric constantϵ_r = 80.2, conductivity σ =0.12 (Ω·m) $^{-1}$, and Zeta potential ζ_0 = −0.1 V. Considering the fabrication, different materials may be used for the top/bottom wall and lateral walls, then one only needs to change the value of the Zeta potential at the corresponding wall. The characteristic size of the cross section of the computational domain sketched in Fig.1 is set to be l = 400 μm, the length of the microchannel covered by the electrodes is $n_l \cdot l$ with n_l representing the fold number, and the length of the inlet and outlet parts of the design domain is equal to l. The Reynolds number and Peclet number of the microflow are respectively calculated to be $Re = \rho Ul/\eta$ and $Pe = Ul/D$, where U is the average velocity at the inlet, D is the mass diffusivity. The computational domain is discretized by 20×20×20 brick elements per cubic space with edge size equals to the characteristic size. In the computational domain, the design domain is set to be the top and bottom surfaces, where positive electrode with specified potential is localized on the top surface and the ground electrode is localized on the bottom surface.

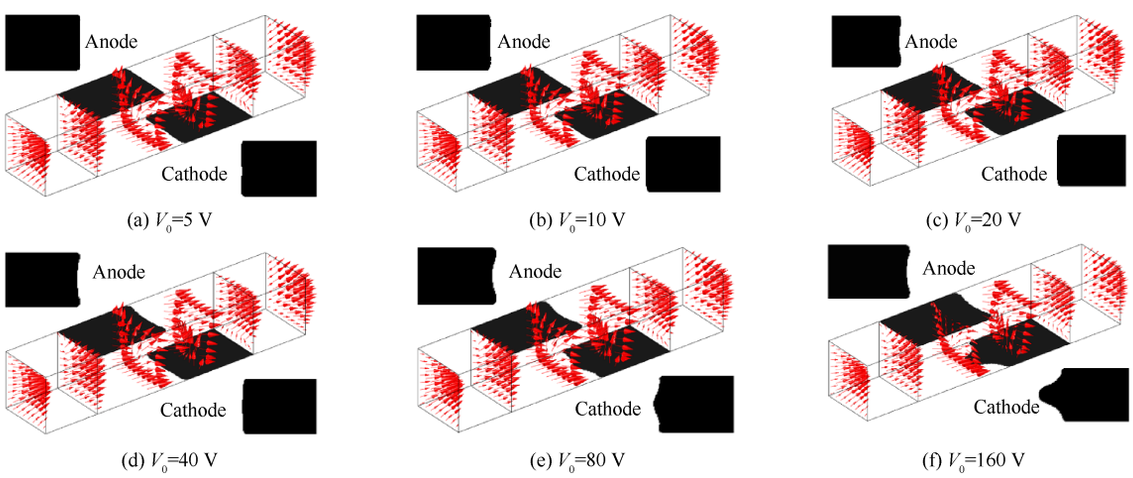

Fig. 2. Topologically optimized layouts for electrodes of electroosmotic micropumps with different actuation potentials.

Based on the introduced topology optimization approach, the electrode layout is investigated in the straight microchannel sketched in Fig. 1 to achieve the micropumping performance. For several different electrical potentials, the layouts of the electrodes are derived as shown in Fig.2(a)-2(f), respectively by setting V_0 to be 5 V, 10 V, 20 V, 40 V, 80 V, and 160 V, where the length of the microchannel covered by the electrodes is 1.2mm with n_l = 3. The red arrows represent the velocity vectors in Fig. 2. And the Reynolds number of the actuated microflows corresponding to different electrical potentials is plotted in Fig.3. Fig.3 shows that the topologically optimized electrode layouts can achieve the increase of the actuated flux of the microflow along with the increase of the imposed electrical potential. The derived electrode layout can control the magnitude of the electric field by adjusting the electric potential, thereby regulating the net flux driving the microchannel.

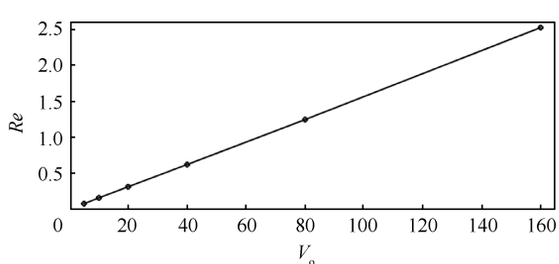

Fig. 3. Plot of actuated Reynolds number corresponding to electroosmotic micropumps.

The distribution of electric field line and velocity are shown in Fig. 4 for the electroosmotic micropump with topologically optimized electrodes and 160 V electrical potential. The electric field lines in Fig.4 shows that the topologically optimized electrodes induce the electric field component in the tangential direction of the microchannel walls. This tangential component actuated the slip velocity at the walls. Because of the viscosity, the fluid in the bulk of the microchannel is actuated sequentially, and this can be confirmed from the velocity distribution shown in Fig. 5. Further, the net flux is generated by the electroosmotic actuation and the topology optimization of the electrode achieve micropump performance.

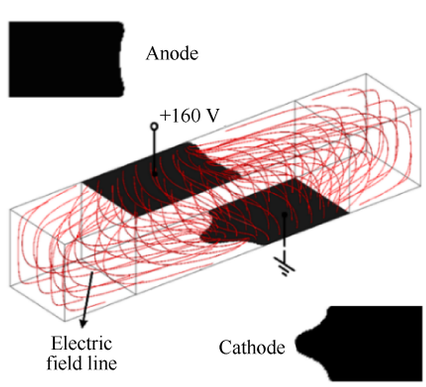

Fig. 4. Electric field line in electroosmotic micropump with topologically optimized electrode layout.

For different length of the pumping microchannel, topology optimization of the electrode layouts is implemented for the electroosmotic micropumps. By setting the fold number of the microchannel length respectively to be different values, the electrode layouts are derived as shown in Fig.6(a)-6(e), where the electrical potential is V_0 = 5 V. The red arrows represent the velocity vectors in Fig.6.The

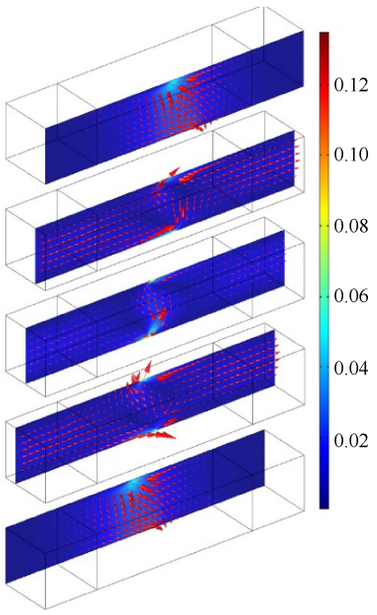

Fig. 5. Distribution of velocity distribution and vectors in cross sections of electroosmotic micropump.

actuated Reynolds number corresponding to the length of the electroosmotic micropumps with the derived electrode layouts are plotted in Fig.7. Fig.7 shows that actuation performance of the topologically optimized electrodes firstly increases along with the increase of the length of the pumping channel, however, its growth rate gradually slowed down, and the driving performance began to decline after reaching a certain pumping channel length. Therefore, relatively longer pumping channel results in larger area of the electrodes, and this is helpful for enhancing the strength of the electric field; as the area of the electrode increases further, a part of the actuation effect of the electric field will be neutralized, then the pumping performance is compromised.

6. Conclusion

This paper has proposed a topology optimization approach for the electrodes of electroosmosis, which is a widespread used actuation mechanism in microfluidics. This approach is implemented based on the interpolation of electric insulation and electric potential on the specified walls of microchannels, where the electrode layouts are determined to achieve the designer desired microfluidic performance. Electroosmotic micropump have been demonstrated as the typical electroosmotic microdevices. Effective pumping of microfluid has been demonstrated with the derived electrodes, where the Reynolds number of the actuated microflows can reach 2.5 with 160 V electrical potential imposed. This approach has the advantage on overcoming the limits of physical intuition-based design method. It can provide a symmetrical approach for the design of electroosmotic microfluidics, with potential applications in chemicals and biochemistry due to the outstanding performance of the derived microdevices. This paper has studied topology optimization of electrode layout for DC electroosmosis with steady microflows, and the AC electroosmosis with unsteady microflows will be investigated in the future.

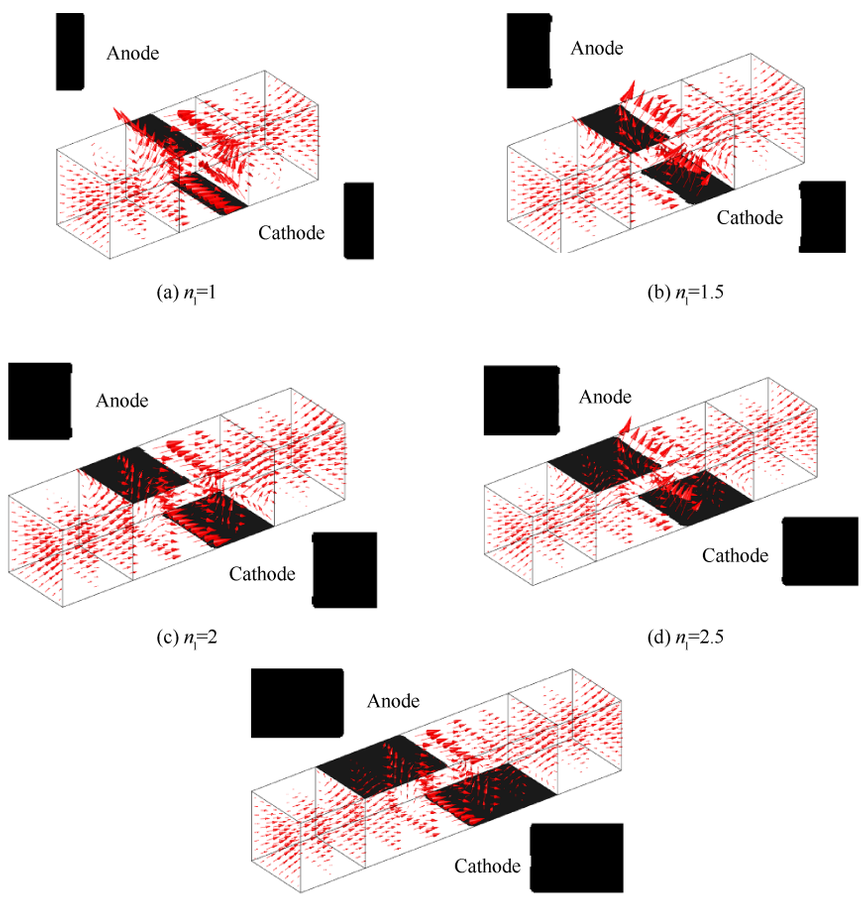

Fig. 6. Topologically optimized layouts for electrodes of electroosmotic micropumps with different length of pumping microchannel.

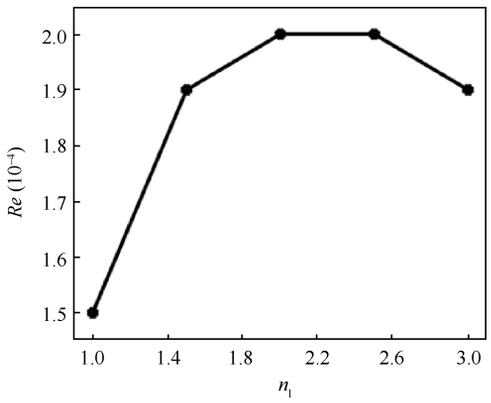

Fig. 7. Plot of actuated Reynolds number corresponding to electroosmotic micropumps.

Acknowledgements

The authors acknowledge the support from the Innovation Grant of Changchun Institute of Optics, Fine Mechanics and Physics (CIOMP), the Fund of State Key Laboratory of Applied Optics (SKLAO), the Youth Innovation Promotion Association of the Chinese Academy of Sciences (No. 2018253), the National Natural Science Foundation of China (No. 51875545). The authors are also grateful to Prof. K. Svanberg of KTH for supplying the codes of the method of moving asymptotes. They are also grateful to the reviewers' kind attention and valuable suggestions.

References

1. Langer R. Biomaterials: status, challenges, and perspectives. *Aiche J* 2000;46(7):1286-1289.
2. Stone HA, Strook AD, Ajdari A. Engineering flows in small devices: Microfluidics toward a lab-on-a-chip. *Aunu Rev Fluid Mech* 2004;36: 381-411.
3. Manz A, Graber N, Widmer HM. Miniaturized total chemical analysis systems: A novel concept for chemical sensing. *Sens. Actuators, B.* 1990;1:244-248.
4. Brask A. *Principles of electroosmotic pumps*. 2002.
5. Wang XY, Cheng C, Wang SL, et al. Electroosmotic pumps and their applications in microfluidic systems. *Microfluid Nanofluidics* 2009;6 (2):145.
6. Zeng SL, Chen CH, Mikkelsen JC Jr, et al. Fabrication and characterization of electroosmotic micropumps. *Sens Actuat B Chem* 2001;79(2-3):107-114.
7. Qian SZ, Bau HH. A chaotic electroosmotic stirrer. *Anal Chem* 2002; 74(15):3616-3625.
8. Zhang JB, He GW, Liu F. Electro-osmotic flow and mixing in heterogeneous microchannels. *Phys Rev E Stat Nonlinear Soft Matter Phys* 2006;73: 056305.
9. Ammam M. Electrophoretic deposition under modulated electric fields: a review. *RSC Adv* 2012;2(20):7633-7646.
10. Hunter R J. *Zeta Potential in Colloid Science: Principles and Applications*. 1981.
11. Cummings EB, Griffiths SK, Nilson RH, et al. Conditions for similitude between the fluid velocity and electric field in electroosmotic flow. *Anal Chem* 2000;72(11):2526-2632.
12. Johnson TJ, Ross D, Locascio LE. Rapid microfluidic mixing. *Anal Chem* 2002;74(1):45-51.
13. Chang CC, Yang RJ. Electrokinetic mixing in microfluidic systems. *Microfluid Nanofluid* 2007;3(5):501-525.
14. Jain M, Yeung A, Nandakumar K. Induced charge electro osmotic mixer: Obstacle shape optimization. *Biomicrofluidics* 2009;3(2):22413.
15. Johnson TJ, Locascio LE. Characterization and optimization of slanted well designs for microfluidic mixing under electroosmotic flow. *Lab Chip* 2002;2(3):135-140.
16. Woo HS, Yoon BJ, Kang IS. Optimization of zeta potential distributions for minimal dispersion in an electroosmotic microchannel. *Int J Heat Mass Transf* 2008;51(17-18):4551-4562.
17. Wu J. Ac electro-osmotic micropump by asymmetric electrode polarization. *J Appl Phys* 2008;103(2):024907.
18. Urbanski JP, Thorsen T, Levitan JA, et al. Fast ac electro-osmotic micropumps with nonplanar electrodes. *Appl Phys Lett* 2006; 89(14): 143508.
19. Matsubara K, Narumi T. Microfluidic mixing using unsteady electroosmotic vortices produced by a staggered array of electrodes. *Chem Eng J* 2016;288: 638-647.
20. Chen JH, Lee YC, Hsieh WH. AC electroosmotic microconcentrator using a face-to-face, asymmetric electrode pair with expanded sections in the bottom electrode. *Microfluid Nanofluid* 2016;20(5):72.
21. Nayak AK, Haque A, Banerjee A, et al. Flow mixing and electric potential effect of binary fluids in micro/nano channels. *Colloids Surf A Physicochem Eng Aspects* 2017;512: 145-157.
22. Risco C, López-Vizcaíno R, Sáez C, et al. Remediation of soils polluted with 2, 4-D by electrokinetic soil flushing with facing rows of electrodes: A case study in a pilot plant. *Chem Eng J* 2016;285: 128-136.
23. Borrvall T, Petersson J. Topology optimization of fluids in Stokes flow. *Int J Numer Methods Fluids* 2003;41(1):77-107.
24. Lazarov B, Sigmund O. Filters in topology optimization based on Helmholtz-type differential equations. *Int J Numer Methods Eng* 2011; 86(6):765-781.
25. Guest J, Prévost J, Belytschko T. Achieving minimum length scale in topology optimization using nodal design variables and projection functions. *Int J Numer Methods Eng* 2004;61(2):238-254.
26. Laser DJ, Santiago JG. A review of micropumps. *J Micromechanics Microengineering* 2004;14: R35-R64.
27. Svanberg K. The method of moving asymptotes—a new method for structural optimization. *Int J Numer Meth Engng* 1987;24(2):359-373.
28. Deng YB, Liu ZY, Zhang P, et al. Topology optimization of unsteady incompressible Navier-Stokes flows. *J Comput Phys* 2011; 230(17): 6688-6708.